Apigenin impairs oral squamous cell carcinoma growth *in vitro* inducing cell cycle arrest and apoptosis

DANIELE MAGGIONI[1], WERNER GARAVELLO[1,2], ROBERTA RIGOLIO[1], LORENZO PIGNATARO[3], RENATO GAINI[1,2] and GABRIELLA NICOLINI[1]

[1]Department of Surgery and Translational Medicine, University of Milan-Bicocca; [2]Department of Otorhinolaryngology, Head and Neck Surgery, San Gerardo Hospital, University of Milan-Bicocca, I-20900 Monza; [3]Department of Clinical Sciences and Community Health, University of Milan, Fondazione IRCCS Ca' Granda Ospedale Maggiore Policlinico, I-20122 Milan, Italy

Received May 10, 2013; Accepted June 21, 2013

DOI: 10.3892/ijo.2013.2072

Abstract. In the present study, we investigated the effect of apigenin, a flavonoid widely present in fruits and vegetables, on a tongue oral cancer-derived cell line (SCC-25) and on a keratinocyte cell line (HaCaT), with the aim of unveiling its antiproliferative mechanisms. The effect of apigenin on cell growth was evaluated by MTT assay, while apoptosis was investigated by phosphatidyl serine membrane translocation and cell cycle distribution by propidium iodide DNA staining through flow cytometry. In addition the expression of cyclins and cyclin-dependent kinases was evaluated by western blotting. A reduction of apigenin-induced cell growth was found in both cell lines, although SCC-25 cells were significantly more sensitive than the immortalized keratinocytes, HaCaT. Moreover, apigenin induced apoptosis and modulated the cell cycle in SCC-25 cells. Apigenin treatment resulted in cell cycle arrest at both G_0/G_1 and G_2/M checkpoints, while western blot analysis revealed the decreased expression of cyclin D_1 and E, and inactivation of CDK1 upon apigenin treatment. These results demonstrate the anticancer potential of apigenin in an oral squamous cell carcinoma cell line, suggesting that it may be a very promising chemopreventive agent due to its cancer cell cytotoxic activity and its ability to act as a cell cycle modulating agent at multiple levels.

Introduction

Oral squamous cell carcinoma (OSCC) is the sixth most widespread cancer with an annual estimated incidence of 263,000 worldwide, two-thirds of these cases occurring in developing countries (1,2). Although its incidence rate is not increasing in the general population of Western countries, an increase in the number of OSCC cases has been reported in young adults in the United States and in some countries of Europe (3-5). The 5-year survival rate remains <60% of diagnosed cases, depending on the stage of the tumor at presentation, in addition, OSCC has devastating consequences negatively affecting the patients quality of life (5). Therefore, developments of new approaches to prevent OSCC occurrence and growth are highly desirable.

Epidemiological studies have identified several nutrients derived from plants with anticancer properties and, among these, flavonoids, a family of polyphenolic compounds, have proved to be effective in cancer prevention (6). Apigenin (Api) is a flavonoid widely found in fruits such as oranges and grapefruits, vegetables and in plant-derived beverages such as chamomile, tea and wine (7). Due to its low toxicity and its biological activities, i.e. anti-inflammatory and anti-oxidant effects, there has been increasing interest in the potential use of Api as an anticancer agent (8). Several studies have proved Api to be effective in inhibiting tumor growth *in vitro* in several types of cancer cells including breast, cervical, prostate and colorectal ones (9-12). The *in vivo* effectiveness of Api oral administration has been demonstrated against prostate cancer (13,14). Moreover, the topical application of Api was found to counteract skin carcinoma growth in mice (15). Although Api has been widely studied the cellular mechanisms responsible of its beneficial effects are still far from being completely understood and scarce information is available regarding the use of Api in oral cancer (16,17). Api anticancer action depends on various mechanisms that can vary according to cell type and it involves apoptosis, modulation of the cell cycle and alteration of kinase pathways (8). Therefore, the aim of the present study is to investigate the anti-proliferative effect of Api on OSCC cells, elucidating the underlying molecular mechanisms. To this end we evaluated Api's effects on tongue derived OSCC cell lines, SCC-25 and on the spontaneously immortalized keratinocytes, HaCaT.

Materials and methods

Cell lines and materials. SCC-25, derived from a human oral squamous cell carcinoma of the tongue (obtained from ATCC,

Correspondence to: Dr Daniele Maggioni, Department of Surgery and Translational Medicine, University of Milan-Bicocca, Via Cadore 48, I-20900 Monza (MB), Italy
E-mail: daniele.maggioni1@unimib.it

Key words: oral squamous cell carcinoma, apigenin, cell cycle, HaCaT and SCC-25

USA) were maintained in DMEM/F12 (Euroclone, Pero, Italy) supplemented with 10% fetal bovine serum (FBS) (Euroclone), 400 ng/ml hydrocortisone (Sigma-Aldrich, St. Louis, MO, USA) and 1% penicillin/streptomycin (Euroclone). HaCaT cells (obtained from German Cancer Research Center, Heidelberg, Germany) were cultured in high glucose DMEM (Euroclone) supplemented with 10% FBS and 1% penicillin/streptomycin. Cells were maintained at 37˚C in a humidified incubator with 5% CO_2. Apigenin (Sigma-Aldrich) was dissolved in pure DMSO and subsequently diluted in culture medium. DMSO concentration did not exceed 0.1% during treatments.

MTT assay. The effect of Api on cell vitality was evaluated by thiazolyl blue tetrazolium bromide (MTT) assay. Cells were transferred to 96-well plates (5,000 cells/cm^2) and were incubated with Api for 24 and 48 hours (h). Subsequently, the medium was removed and the cells were incubated with MTT (Sigma-Aldrich). Four hours later, formazan crystals were dissolved with DMSO and the absorbance was recorded at 560 nm in a microplate reader (Bio-Rad, Hercules, CA, USA). The effect of Api on cell survival was calculated by normalizing the data to the absorbance of vehicle-treated cells (considered as 100%). The IC_{50} value was estimated.

Annexin V-propidium iodide assay. In order to evaluate Api-induced apoptosis, the FITC conjugated Annexin V-propidium iodide (PI) apoptosis detection kit (BD Biosciences, Buccinasco, Italy) was used according to the manufacturer's instructions. Briefly, the cells were plated in 6-well plates (5,000 cells/cm^2) and treated for 24 h with Api 100 μM. Both floating and attached cells were harvested, washed with PBS and, finally, suspended in binding buffer containing Annexin V and PI. After 15-min incubation in the dark, the presence of apoptotic cells was analysed by the FACSCantoI flow cytometer (BD Biosciences).

Analysis of cell cycle distribution. After Api treatment, both floating and attached cells were harvested, washed twice with cold PBS, spun in a refrigerated centrifuge at 200 g for 10 min and resuspended in cold 70% ethanol overnight (ON) at 4˚C. The following day the cells were washed in cold PBS and then incubated in 5 μg/ml PI and 12.5 μg/ml RNAse (both from Sigma-Aldrich) for 48 h. When the cell synchronization was required, SCC-25 and HaCaT cells were maintained in serum-free medium for 30 and 48 h, respectively, and subsequently treated with Api in complete medium. DNA content analysis was subsequently performed by means of a FACSCantoI flow cytometer (BD Biosciences, Buccinasco, Italy) and ≥20,000 events were analyzed. Cell cycle distribution was then analyzed by ModFit LT (Verity House Software, Topsham, ME, USA).

Western blotting. The Api-treated and control cells were washed twice in cold PBS and lysed in 50 mM HEPES, pH 7.5, 150 mM NaCl, 10% glycerol, 1% Triton X-100, 1.5 mM $MgCl_2$, 5 mM EGTA, 4 mM phenylmethylsulfonyl fluoride, 1% aprotinin, 10 mM sodium orthovanadate, 20 mM sodium pyrophosphate (all from Sigma-Aldrich). The lysates were clarified by centrifugation at 13,000 g for 15 min at 4˚C and the total protein content was evaluated with a Coomassie Protein Assay Reagent kit (Pierce, Rockford, IL, USA). Cell lysates (50 μg), mixed with Laemmli buffer (5% β-mercaptoethanol, 10% SDS, 50% glycerol, 400 mM Tris-HCl (pH 6.8) and 0.5% bromophenol blue) (all from Sigma-Aldrich), were resolved overnight in a 13% SDS-PAGE and then electroblotted onto nitrocellulose membranes (GE Healthcare Life Science, Milan, Italy).

Non-specific binding sites were blocked by 1 h room temperature (RT) incubation in 5% non-fat milk in TBS (10 mM Tris-HCl pH 8, 150 mM NaCl, 0.05% Tween-20). Subsequently, membranes were incubated overnight with the following primary antibodies diluted in TBS plus 5% non-fat milk: cyclin D_1, cyclin E (Santa Cruz Biotechnology, Santa Cruz, CA, USA), Actin (Santa Cruz Biotechnology), cyclin-dependent kinase 1 (CDK1), phospho-CDK1 (Cell Signaling Technology, Danvers, CA, USA). Unbound antibodies were removed by TBS washing and the membranes were subsequently incubated with peroxidase-conjugated specific secondary antibodies for 1 h at RT. Finally, the immune complexes were visualized using an enhanced chemiluminescence (ECL) system (Genespin Srl., Milan, Italy). After blot scanning, the densitometric analysis of the bands was performed using the Gel Logic 100 Imaging System (Eastman Kodak, Rochester, NY, USA). Results were expressed as a relative optical density (OD) considering the ratio between the optical density of the protein band of interest and that of the corresponding actin band.

Statistical analysis. Data are reported as means ± standard deviation from at least three independent experiments. The statistical evaluation of the results was performed using GraphPad Prism 3 Software (GraphPad Softwar Inc., La Jolla, CA, USA). The differences between controls and treated cell MTT results were analyzed by the one-way ANOVA analysis of variance followed by Dunnett's multiple comparison test. Differences in the percentages of apoptotic cells in the Annexin V-PI assay and differences in the cell cycle distribution between controls and treated cells were analyzed by Student's t-test. Statistical significance was set at $p<0.05$.

Results

Apigenin treatment inhibits cell proliferation. The effect of different Api concentrations on cell survival was evaluated using MTT assay. The data obtained showed a dose- and time-dependent decrease in cell vitality in both HaCaT and SCC-25 cells (Fig. 1).

As can be observed in the graph of Fig. 1A, the highest doses of Api used induced a marked, statistically significant, decrease in SCC-25 cells survival after 24-h treatment, in particular Api 50 and 100 μM reduced cell viability to values <50% with respect to untreated controls. The Api-induced decrease in cell viability was observed also in HaCaT cells; however, the effect of Api in these cells was milder than in SCC-25 cells, in fact, only Api 100 μM significantly affected HaCaT cell viability.

After 48-h treatment all the tested doses statistically significantly reduced SCC-25 cells viability, in particular a dramatic drop in cell vitality to 18.1±7.% and 7.9±2.0%

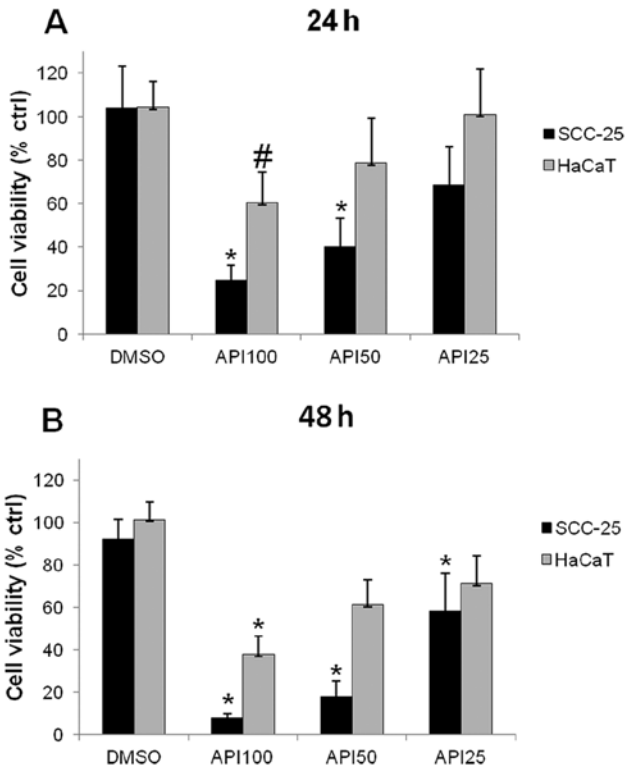

Figure 1. Effect of apigenin on cell survival. Cells were treated with DMSO 0.1% or Api (25, 50 and 100 μM) and incubated for 24 and 48 h. (A) SCC-25 cells. (B) HaCaT cells. Cell survival was evaluated by MTT assay. Data represent percentages of cell viability in comparison to untreated control cells that were arbitrarily set to 100% and are reported as the means ± SD of three independent experiments. $^{\#}$p<0.05; *p<0.01 versus vehicle-treated group, one-way ANOVA, Dunnett's post-test.

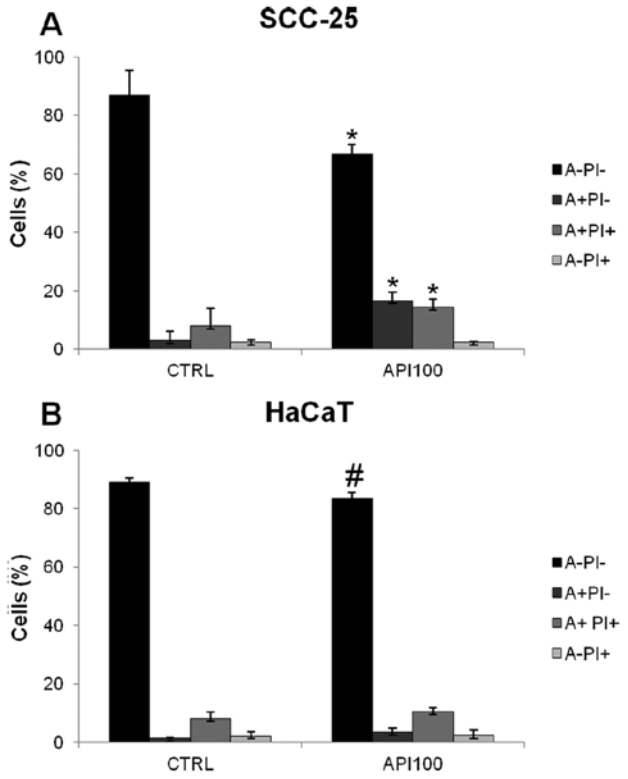

Figure 2. Analysis of apoptosis by Annexin V (A)/propidium iodide (PI) staining. SCC-25 (A) and HaCaT cells (B) were incubated with 100 μM Api for 24 h and then stained with FITC conjugated Annexin V and propidium iodide. Live cells are A^-P^-, early apoptotic cells are A^+PI^-, cells late in apoptosis or necrotic cells are A^+PI^+, while necrotic cells are A^-PI^+. Data represent percentages of cells, reported as means ± SD of three independent experiments. $^{\#}$p<0.05; *p<0.01 versus CTRL, Student's t-test.

was observed after 48-h treatment with 50 and 100 μM Api, respectively. The Api-induced decrease in cell viability with respect to vehicle-treated cells was observed also in HaCaT cells; however, the effect of Api in these cells was milder than in SCC-25 cells, in fact, only Api 100 μM reduced HaCat cell viability below 50% (Fig. 1B).

Apigenin induces apoptosis in SCC-25 cells. To assess if the Api-induced decrease in cell survival was related to apoptosis, we performed a flow cytometric analysis of the membrane translocation of phosphatidyl serine with FITC-conjugated Annexin V (A), combined with PI DNA staining (PI). As shown in Fig. 2A, 24 h exposure to 100 μM Api significantly increased the percentage of apoptotic SCC-25 cells (A^+/PI^-). In particular, the population of cells showing A^+/PI^- increased from <1.47±0.78% in the controls to 19.8±4.1% in Api-treated cells (p<0.01), whereas the percentage of cells in late apoptosis, being positive for both Annexin V and PI staining (A^+/PI^+), increased from 4.73±0.74 in the controls to 14.6±2.05% in Api-treated cells (p<0.01) (Fig. 2A). On the contrary, 100 μM Api treatment induced only a slight, statistically insignificant, increase in the percentage of early and late apoptotic cell populations in HaCaT cells (Fig. 2B).

Cell cycle alteration induced by apigenin. We aimed at correlating the Api-induced inhibition of cell growth with an alteration of the cell cycle progression. Therefore, we performed cell cycle analysis in cells treated with the most effective dose of Api (100 μM) for 24 and 48 h.

An increase in the percentage of cells in the G_2/M phase in Api-treated cells was observed in both HaCaT and SCC-25 cells compared with untreated controls. This increase was associated with a slight, but statistically significant, decrease in the percentage of cells in both G_0/G_1 and S phase after 48 h exposure. The modulation of SCC-25 cell cycle distribution due to Api, although already notable after 24 h Api exposure, became statistically significant after 48 h (Fig. 3A), so that Api 100 μM treatment resulted in 48.2±4% of cells in G_2/M, versus the 9.3±0.8% observed in controls (Fig. 3A). In HaCaT cells, 48 h Api treatment resulted in an increase in the G_2/M population from 7.1±1.7 in controls to 26.1±1 % in treated cells (p<0.001) (Fig. 3B).

Despite the increase in the G_2/M population, there was a considerable number of cells still in the G_0/G_1 phase, thus suggesting that another checkpoint might be involved in Api-induced modulation of cell cycle progression. In an attempt to better clarify the effect of Api on cell cycle distribution, we analyzed the effect of 100 μM Api on synchronized cells. For this purpose, SCC-25 and HaCaT cells were maintained in serum-free medium for 30 and 48 h, respectively, then cells were allowed to re-enter the cell cycle by culturing them in complete medium. As shown in Fig. 4, we obtained

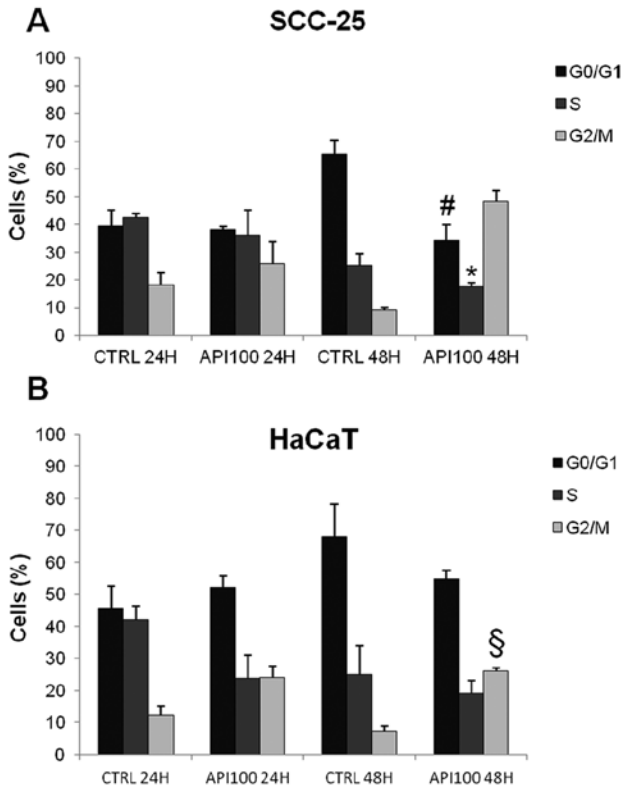

Figure 3. Effect of Api on cell cycle distribution in unsynchronized cells. SCC-25 cells (A) and HaCaT cells (B) were treated with 100 μM Api for 24 and 48 h. Data represent percentages of cells in G_0/G_1, S and G_2/M phases and are reported as the means ± SD of three independent experiments. $^{\#}p<0.05$ versus CTRL 48 h; $^{*}p<0.01$ versus CTRL 48 h; $^{\S}p<0.001$ versus CTRL 48H, Student's t-test.

satisfactory synchronization, with almost 90% of cells being in the G_0/G_1 phase following serum starvation. Api treatment on synchronized HaCaT and SCC-25 cells resulted in the maintainance of cells into the G_0/G_1 phase, in fact, while in untreated controls the majority of cells after 24 h were in the S phase as a result of cycle re-entering after serum starvation, Api-treated cells maintained the same distribution of serum starvation synchronized cells both after 24 and 48 h of treatment (Fig. 4). In synchronized SCC-25 cells, the exposure to 100 μM Api for 24 h resulted in 85.7±11.5% of cells being in G_0/G_1 ($p<0.01$ versus controls) and a very similar effect was observed in HaCaT cells. The blockage of cells in G_0/G_1 persisted also after 48 h treatment. Despite this, the blockage at G_2/M transition was still evident in HaCaT cells since a slight, but statistically significant ($p<0.01$), increase in the percentage of cells in G_2/M was found in 24 h Api-treated cells when compared to controls.

Apigenin inactivates CDK1 in SCC-25 cells. In order to address in more detail the effect of Api on the cell cycle, we evaluated the expression of some cyclins and the associated CDKs that regulate both G_0/G_1 and G_2/M phase transition.

Therefore, we considered the protein level of cyclin B1, which is involved in G_2/M transition, in unsynchronized cells. However, no significant modulations of its expression by Api were evidenced either in SCC-25 or in HaCaT cell lines (data not shown). We subsequently evaluated the level of the CDK1, also known as $p34^{cdc2}$, which is functionally associated with cyclin B1. Even in this case we did not observe any variation/modulation between treated and control cells. Nevertheless

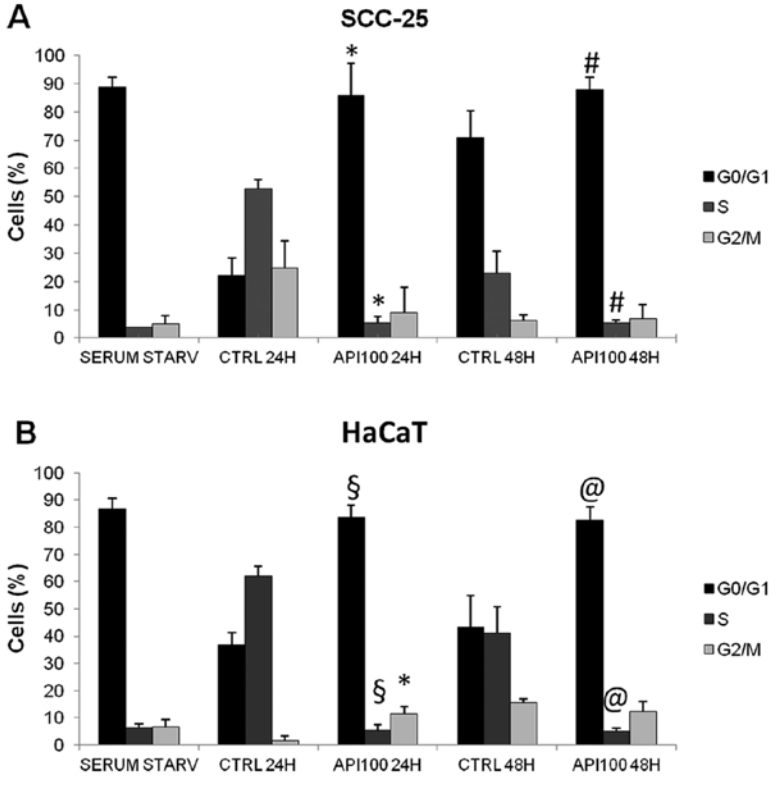

Figure 4. Effect of Api on the cell cycle distribution in synchronized cells. SCC-25 cells (A) and HaCaT cells (B) were synchronized by serum starvation for 30 and 48 h, respectively. Subsequently cells were treated with 100 μM Api in complete medium for 24 and 48 h. Data represent percentage of cells in G_0/G_1, S and G_2/M phases and are reported as the means ± SD of three independent experiments. $^{\#}p<0.05$ versus CTRL 48 h; $^{*}p<0.01$ versus CTRL 24 h; $^{@}p<0.01$ versus CTRL 48 h, $^{\S}p<0.001$ versus CTRL 24 h, Student's t-test.

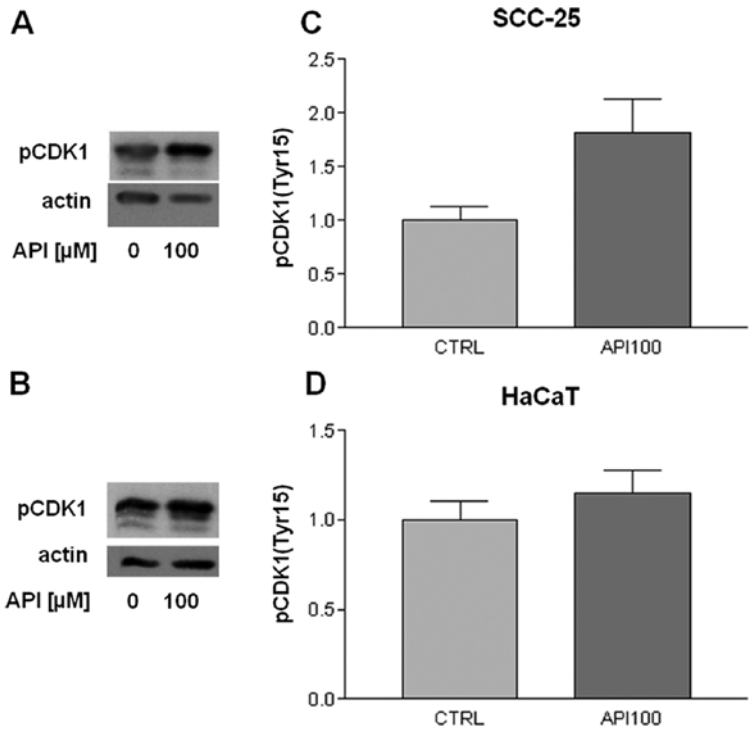

Figure 5. Effect of Api on tyrosine 15 phosphorylated CDK1 (pCDK1) expression. Cells were cultivated for 24 h in the presence of 100 μM Api (A100), control is represented by untreated cells (CTRL). Representative western blot showing protein level of pCDK1 in SCC-25 cells (A) and in HaCaT cells (B). Anti-actin immunoblotting was performed as internal loading control. Graphs show the relative levels of optical density of pCDK1 bands normalized to the expression of actin in SCC-25 cells (C) and in HaCaT cells (D). Data are reported as means ± SD of three independent experiments.

the regulation of CDK1 is quite complex; in fact, it is strictly regulated by phosphorylation so that its enzimatic activity is inhibited by phosphorylation on the tyrosine in position 15. Therefore, we evaluated the level of the tyrosine 15 phosphorylated form of CDK1. As shown in Fig. 5, a marked, although not statistically significant, increase in tyrosine 15 phosphorylated CDK1 was observed in SCC-25 cells following 100 μM Api treatment for 24 h (Fig. 5C), whereas Api treatment did not modulate the level of tyrosine 15 phosphorylation in HaCaT cells (Fig. 5D).

Apigenin modulates cyclin D_1 and E expression. In view of the different Api action on the cell cycle in synchronized versus asynchronous cells, we analyzed also the cyclins and CDKs involved in the regulation of G_0/G_1 transition in synchronized cells. First, we evaluated the expression of cyclin D_1, which drives the progression through the G_1 phase of cell cycle, by exposing synchronized cells to 100 μM Api for 24 h. As can be seen in Fig. 6, Api treatment modulated cyclin D_1 expression in both cell lines, with a statistically significant decrease being observed in SCC-25 cells (Fig. 6C), while the decrease in cyclin D_1 was slight in HaCaT cells (Fig. 6B and D). Secondly, we evaluated the Api effect on the expression of cyclin E, whose levels are generally high during the mid G_1 phase and which is involved in the regulation of G_1/S transition. We did not find any cyclin E expression in SCC-25 cells (data not shown). On the contrary, a statistically significant decrease in HaCaT cells after Api treatment was found. The level of cyclin E expression significantly dropped after 24 h Api treatment in HaCaT cells (Fig. 7).

Discussion

Apigenin, a flavonoid belonging to the class of flavones has proved its effectiveness against various cancer types (8-13), but up to now scarce data are available regarding the Api effects and molecular mechanisms on OSCC.

In the present study, we aimed at evaluating Api's action on OSCC using the cell line SCC-25, derived from tongue OSCC. In addition, Api's effect was analyzed also on a spontaneously immortalized, non-tumorigenic, keratinocyte cell line: HaCaT cells. These cell lines have been widely used and they represent a valid model for studying the action of potential chemotherapeutic agents (18,19). In addition, HaCaT cells may be considered a good model of the initial transformation of squamous cell carcinoma. In fact, although they can be referred to as normal keratinocytes, they show some molecular alterations, found in the first steps of malignant transformation of epithelial cells, such as the mutations in both p53 alleles (20).

We demonstrated that Api inhibits cancer cell growth *in vitro*; it was able to significantly decrease cell survival in SCC-25 cells. In our paradigm, the SCC-25 cells were much more sensitive to Api than immortalized keratinocytes (HaCaT). In agreement with our findings a selective growth inhibitory effect of Api in prostate cancer cells when compared with non-transformed cells was reported (9). Masuelli and colleagues (17) also reported a comparable proliferation inhibition in SCC-15, OSCC derived cells.

Consistent with data reported in breast (10) and in lung cancer (21), the analysis of the phosphatidyl serine membrane

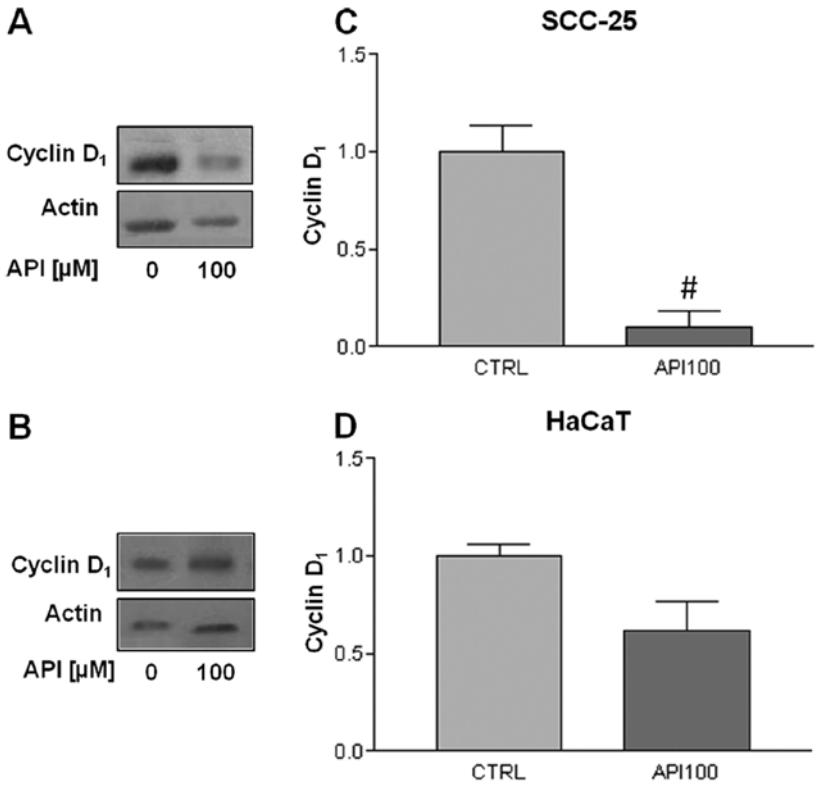

Figure 6. Api effect on cyclin D_1 expression in synchronized cells. Cells were cultivated for 24 h in the presence of 100 μM Api (A100), control is represented by untreated cells (CTRL). Representative western blot showing protein level of cyclin D_1 in SCC-25 cells (A) and in HaCaT cells (B). Anti-actin immunoblotting was performed as internal loading control. Graphs show the average levels of cyclin D_1 in SCC-25 cells (C) and in HaCaT cells (D), expressed as relative level of optical density of cyclin D_1 bands normalized to the expression of actin and they are reported as the means ± SD of three independent experiments. $^{\#}p<0.05$ versus CTRL, Student's t-test.

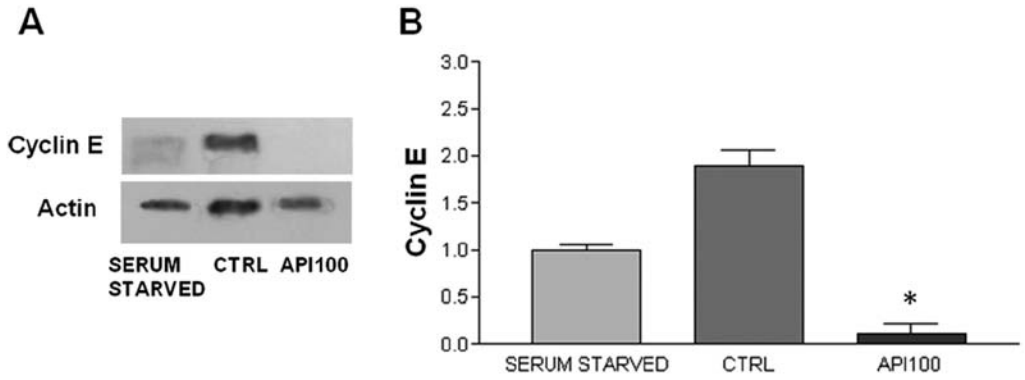

Figure 7. Api effect on cyclin E expression in HaCaT cells. (A) Representative western blot showing protein levels of cyclin E. Cells were synchronized by serum starvation for 48 h and subsequently treated with 100 μM Api (A100) in complete medium for 24 h. Controls (CTRL) are synchronized cells that did not receive Api. Anti-actin immunoblotting was performed as internal loading control. (B) Graphs show the relative levels of optical density of cyclin E bands normalized to the expression of actin. Data are reported as the means ± SD of three independent experiments. $^{*}p<0.01$ versus CTRL, one-way ANOVA test, Tukey's post-test.

translocation, an early apoptotic marker, showed that Api induced apoptosis in SCC-25 cells. Apoptosis was not detected in HaCaT cells, thus confirming a selective cytotoxic action of Api towards tumoral SCC-25 cells. The absence of apoptosis in HaCaT cells is not in agreement with previously reported data from Abu-Yousif *et al* (22), where the exposure of HaCaT cells to Api led to apoptosis in almost 15% of cells. One possible reason for this difference might be that in the study of Abu-Yousif *et al* Api treatment was conducted in serum-free medium, while in the present study HaCaT cells were maintained in complete medium during evaluation of Api cytotoxicity. However, the ratio of apoptotic cells alone was not enough to explain the decrease in cell viability observed in SCC-25 cells following Api treatment. Furthermore, the absence of apoptosis in HaCaT cells, whose proliferation was inhibited by Api, led us to hypothesize that mechanisms other

than apoptosis had a role in the cell number decrease observed after Api treatment. We therefore investigated whether the impairment of cell growth was associated with alterations in the cell cycle progression. The analysis of cell cycle distribution showed a marked increase in the percentage of cells in the G_2/M phase after Api treatment in both cell lines. These results are in agreement with data reported by Ujiki *et al* (23) and Choi and Kim (10) that demonstrated an Api-induced G_2/M arrest in pancreatic and breast cancer cells, respectively. In addition, an increase in the G_2/M population after Api exposure was observed also in immortalized keratinocytes (24,25) and in primary cultures of OSCC (16). On the contrary, our results differ from the data reported by Masuelli and co-workers (17). Although they reported an Api-induced decrease in cell survival similar to our findings, they found a significant decrease in cells in both G_1 and G_2/M phases after Api exposure in SCC-15. The main regulator of G_2/M progression is the CDK1/cyclin B complex whose activity is required for cells to enter mitosis. In our paradigm, Api induced only a slight modulation of the level of cyclin B and CDK1 (data not shown). However, CDK1 activity is also regulated by phosphorylation and dephosphorylation mediated by wee1 and cdc25 and, in particular dephosphorylation of CDK1 at the tyrosine 15 site is required for its activity (26). Api treatment induced a significant increase in the level of tyrosine 15 phosphorylated CDK1 in SCC-25 cells, thus indicating that Api can inactivate this CDK. Similar results were obtained in human melanoma cells (27). Api's ability to inactivate CDK1 through phosphorylation on tyrosine 15 sites was demonstrated also by McVean *et al* (25) in epidermal keratinocytes. On the contrary, HaCaT cells did not show any modulation of CDK1 phosphorylation after Api treatment, thus indicating that Api induces G_2/M arrest through of different mechanisms in different cell types.

Even after 48 h Api exposure, a relatively large percentage of cells still remained in the G_0/G_1 phase leading us to hypothesize that Api could also impair G_1 progression. Api treatment in synchronized cells resulted in an almost complete G_0/G_1 arrest in both the cell lines. These data are consistent with results by Lepley and Pelling (28) who reported a G_1 accumulation in synchronized skin fibroblasts exposed to Api, while unsynchronized cells were arrested in G_2/M. Western blot analysis demonstrated that Api-induced G_0/G_1 arrest depended on different pathways in SCC-25 and HaCaT cells. A statistically significant decrease in the expression of the cyclin E cell was found in HaCaT, whereas we found no expression of this cyclin in SCC-25 cells, although cyclin E overexpression is often found in oral cancer (29). However, the loss of cyclin E expression has been reported in two other tongue-derived SCC cell lines (30). It is, therefore, conceivable that cell growth deregulation in SCC-25 cells might depend on the loss of cyclin E. These observations suggest that Api has a double action on the cell cycle, inducing both a G_0/G_1 and a G_2/M arrest, accompanied by a reduction in cyclin D_1 and cyclin E expression and inactivation of CDK1.

In conclusion, we demonstrated an inhibitory effect on cell survival and apoptotic effect of Api in oral cancer cells. The model of action we hypothesize implies the induction of apoptosis in SCC-25 cells by Api, which also determines the cell cycle arrest acting as a CDK1 inhibitor and inducing a decrease in cyclin D_1 expression.

Therefore, it appears that Api deserves to be further studied as a potential agent for oral cancer prevention and treatment since it is able to induce cell cycle arrest and apoptosis in OSCC cells. In addition, Api seems to be a very promising cell cycle regulating agent since it is able to induce a double cell cycle arrest in different phases. It could, therefore, be capable of arresting cell cycle progression also in cells, such as SCC-25 where the cycle regulation machinery is deregulated but not completely compromised.

References

1. Jemal A, Siegel R, Xu J and Ward E: Cancer statistics. CA Cancer J Clin 60: 277-300, 2010.
2. Garavello W, Bertuccio P, Levi F, Lucchini F, Bosetti C, Malvezzi M, Negri E, La Vecchia C: The oral cancer epidemic in central and eastern Europe. Int J Cancer 127: 160-171, 2010.
3. Shiboski CH, Schmidt BL and Jordan RC: Tongue and tonsilar carcinoma: increasing trends in the US population ages 20-44 years. Cancer 103: 1843-1849, 2005.
4. Bonifazi M, Malvezzi M, Bertuccio P, Edefonti V, Garavello W, Levi F, La Vecchia C, Negri E: Age-period-cohort analysis of oral cancer mortality in Europe: the end of an epidemic? Oral Oncol 47: 400-407, 2011.
5. Warnakulasuriya S: Living with oral cancer: epidemiology with particular reference to prevalence and life-style changes that influence survival. Oral Oncol 46: 407-410, 2010.
6. Rossi M, Garavello W, Talamini R, Negri E, Bosetti C, Dal Maso L, Lagiou P, Tavani A, Polesel J, Barzan L, Ramazzotti V, Franceschi S, La Vecchia C: Flavonoids and the risk of oral and pharyngeal cancer: a case-control study from Italy. Cancer Epidemiol Biomarkers Prev 16: 1621-1625, 2007.
7. Shukla S and Gupta S: Apigenin: a promising molecule for cancer prevention. Pharm Res 27: 962-978, 2010.
8. Patel D, Shukla S and Gupta S: Apigenin and cancer chemoprevention: progress, potential and promise (Review). Int J Oncol 30: 233-245, 2007.
9. Gupta S, Afaq F and Mukhtar H: Selective growth-inhibitory, cell-cycle deregulatory and apoptotic response of apigenin in normal versus human prostate carcinoma cells. Biochem Biophys Res Commun 287: 914-920, 2001.
10. Choi EJ and Kim GH: Apigenin induces apoptosis through a mtochondria/caspase-pathway in human breast cancer MDA-MB-453 cells. J Clin Biochem Nutr 44: 260-265, 2009.
11. Zhong Y, Krisanapun C, Lee SH, Nualsanit T, Sams C, Peungvicha P and Baek SJ: Molecular targets of apigenin in colorectal cancer cells: involvement of p21, NAG-1 and p53. Eur J Cancer 46: 3365-3374, 2010.
12. Xu Y, Xin Y, Diao Y, Lu C, Fu J, Luo L and Yin Z: Synergistic effects of apigenin and paclitaxel on apoptosis of cancer cells. PLoS One 6: e29169, 2011.
13. Kaur P, Shukla S and Gupta S: Plant flavonoid apigenin inactivates Akt to trigger apoptosis in human prostate cancer: an in vitro and in vivo study. Carcinogenesis 29: 2210-2217, 2008.
14. Pandey M , Kaur P, Shukla S, Abbas A, Fu P and Gupta S: Plant flavone apigenin inhibits HDAC and remodels chromatin to induce growth arrest and apoptosis in human prostate cancer cells: in vitro and in vivo study. Mol Carcinog 51: 952-962, 2012.
15. Wei H, Tye L, Bresnick E and Birt DF: Inhibitory effect of apigenin, a plant flavonoid, on epidermal ornithine decarboxylase and skin tumor promotion in mice. Cancer Res 50: 499-502, 1990.
16. O'Prey J, Brown J, Fleming J and Harrison PR: Effects of dietary flavonoids on major signal transduction pathways in human epithelial cells. Biochem Pharmacol 66: 2075-2088, 2003.
17. Masuelli L, Marzocchella L, Quaranta A, Palumbo C, Pompa G, Izzi V, Canini A, Modesti A, Galvano F and Bei R: Apigenin induces apoptosis and impairs head and neck carcinomas EGFR/ErbB2 signaling. Front Biosci 16: 1060-1068, 2011.
18. Scott RE, Wilke MS, Wille JJ Jr, Pittelkow MR, Hsu BM and Kasperbauer JL: Human squamous carcinoma cells express complex defects in the control of proliferation and differentiation. Am J Pathol 133: 374-380, 1988.
19. Boukamp P, Petrussevska RT, Breitkreutz D, Hornung J, Markham A and Fusenig NE: Normal keratinization in a spontaneously immortalized aneuploid human keratinocyte cell line. J Cell Biol 106: 761-771, 1988.

20. Komissarova EV and Rossman TG: Arsenite induced poly(ADP-ribosyl)ation of tumor suppressor P53 in human skin keratinocytes as a possible mechanism for carcinogenesis associated with arsenic exposure. Toxicol Appl Pharmacol 243: 399-404, 2010.
21. Lu HF, Chie YJ, Yang MS, Lee CS, Fu JJ, Yang JS, Tan TW, Wu SH, Ma YS, Ip SW and Chung JG: Apigenin induces caspase-dependent apoptosis in human lung cancer A549 cells through Bax- and Bcl-2-triggered mitochondrial pathway. Int J Oncol 36: 1477-1484, 2010.
22. Abu-Yousif AO, Smith KA, Getsios S, Green KJ, Van Dross RT and Pelling JC: Enhancement of UVB-induced apoptosis by apigenin in human keratinocytes and organotypic keratinocyte cultures. Cancer Res 68: 3057-3065, 2008.
23. Ujiki MB, Ding XZ, Salabat MR, Bentrem DJ, Golkar L, Milam B, Talamonti MS, Bell RH Jr, Iwamura T and Adrian TE: Apigenin inhibits pancreatic cancer cell proliferation through G2/M cell cycle arrest. Mol Cancer 5: 76, 2006.
24. Lepley DM, Li B, Birt DF and Pelling JC: The chemopreventive flavonoid apigenin induces G2/M arrest in keratinocytes. Carcinogenesis 17: 2367-2375, 1996.
25. McVean M, Weinberg WC and Pelling JC: A p21(waf1)-independent pathway for inhibitory phosphorylation of cyclin-dependent kinase p34(cdc2) and concomitant G(2)/M arrest by the chemopreventive flavonoid apigenin. Mol Carcinog 33: 36-43, 2002.
26. Parker LL and Piwnica-Worms H: Inactivation of the p34cdc2-cyclin B complex by the human WEE1 tyrosine kinase. Science 257: 1955-1957, 1992.
27. Casagrande F and Darbon JM: Effects of structurally related flavonoids on cell cycle progression of human melanoma cells: regulation of cyclin-dependent kinases CDK2 and CDK1. Biochem Pharmacol 61: 1205-1215, 2001.
28 Lepley DM and Pelling JC: Induction of p21/WAF1 and G1 cell-cycle arrest by the chemopreventive agent apigenin. Mol Carcinog 19: 74-82, 1997.
29. Shintani S, Mihara M, Nakahara Y, Kiyota A, Ueyama Y, Matsumura T and Wong DT: Expression of cell cycle control proteins in normal epithelium, premalignant and malignant lesions of oral cavity. Oral Oncol 38: 235-243, 2002.
30. Yamada S, Sumrejkanchanakij P, Amagasa T and Ikeda MA: Loss of cyclin E requirement in cell growth of an oral squamous cell carcinoma cell line implies deregulation of its downstream pathway. Int J Cancer 111: 17-22, 2004.